

Mott Gap Excitation and Resonant Inelastic X-Ray Scattering in Doped Cuprates

Kenji Tsuchi, Takami Tohyama, and Sadamichi Makiawa
 Institute for Materials Research, Tohoku University, Sendai 980-8577, Japan
 (Dated: October 13, 2019)

It is proposed by using the numerically exact diagonalization technique for the two-dimensional Hubbard model with second and third neighbor hopping terms that momentum- and carrier-dependent degradation of the Mott gap upon doping in high- T_c cuprates is grasped in the Cu K-edge resonant X-ray scattering (RIXS). Special emphasis is placed in the asymmetry between electron- and hole-carriers. We argue that the Mott gap excitation observed by RIXS is strongly affected by the interaction between charge carriers and antiferromagnetic correlations as like the low-energy properties.

PACS numbers: 74.25.Jb, 71.10.Fd, 78.70.Ck

Resonant inelastic x-ray scattering (RIXS) is growing as a powerful technique to investigate elementary excitations in strongly correlated electron systems such as high- T_c cuprates. The Cu K-edge RIXS measurements on two-dimensional insulating cuprates [1, 2] have been carried out and revealed the momentum dependence of the charge-transfer process from the occupied Zhang-Rice singlet band (ZRB) [3] composed of Cu $3d_{x^2-y^2}$ and O $2p$ orbitals to the unoccupied upper Hubbard band (UHB) [4], i.e., Mott gap excitation. It has been discussed that the antiferromagnetic (AF) correlation in the ground state plays an important role in the characteristic momentum dependence of the RIXS spectra [4, 5]. In addition, the RIXS on one-dimensional insulating cuprates SrCuO_2 and Sr_2CuO_3 have been measured and demonstrated that the character of the separation for the spin and charge degrees of freedom in one dimension appears in RIXS spectrum [6, 7]. These studies on the insulating cuprates indicate that the RIXS measurement can reveal the novel physics associated with the Mott gap excitations.

There is an asymmetry in the electronic properties between electron- and hole-doped cuprates, and it is one of the key issues for clarifying the mechanism of high- T_c superconductivity. In high- T_c cuprates, the antiferromagnetism remains stronger upon electron-doping than hole-doping [8]: In the electron-doped $\text{Nd}_{2-x}\text{Ce}_x\text{CuO}_4$ (NCCO), the antiferromagnetism continues up to $x=0.15$, whereas it disappears with small amount of x (<0.02) in hole-doped $\text{La}_{2-x}\text{Sr}_x\text{CuO}_4$ (LSCO). Physical properties depending on the kind of carriers appear not only in such magnetism but also in the single-particle excitations. High resolution angle-resolved photoemission spectroscopy (ARPES) experiments have revealed that the minimum excitation energy appears at around (π, π) for hole-doping, whereas it does at around $(\pi, 0)$ for electron-doping [9]. On the other hand, the excitations across the Mott gap seen in the optical conductivity showed similar behavior between electron- and hole-dopings [10, 11]. It is, thus, interesting to clarify whether the asymmetry for dopings exist even in high energy region, and how the Mott gap excitation in doped cuprates looks in RIXS.

In this Letter, we demonstrate theoretically the difference of the Cu K-edge RIXS between hole- and electron-doped cuprates. The single-band Hubbard model is adopted to describe the ZRB and UHB by mapping ZRB onto the lower Hubbard band (LHB) in the model. Then, the Cu $1s$ and $4p$ orbitals are incorporated with the model to include the $1s$ -core hole and excited $4p$ electron into the intermediate state of the RIXS process. The long-range hoppings are also introduced in the Hubbard model. The RIXS spectra are calculated by using the numerically exact diagonalization technique. We find that the excitation spectrum from the LHB to the UHB becomes broad and less momentum dependent upon hole-doping. This is in contrast to the case of electron-doping, where the momentum dependence of the spectrum of undoped system remains, except that along the $(\pi, 0)$ direction. The difference in the spectra between hole- and electron-doped systems is found to be related with short-range AF spin correlation in the ground states. We also find that the momentum dependence along the $(\pi, 0)$ direction in electron doping comes from the fact that the doped electrons occupy the states at around $k=(\pi, 0)$ in the upper Hubbard band.

By mapping the ZRB onto the LHB, which is equivalent to the elimination of O $2p$ orbitals [4], the Hubbard Hamiltonian with second and third neighbor hoppings is written as

$$H_{3d} = \sum_{\langle ij \rangle} t_{ij} d_i^\dagger d_j + \sum_{\langle\langle ij \rangle\rangle} t_{ij}^0 d_i^\dagger d_j + \sum_{\langle\langle\langle ij \rangle\rangle\rangle} t_{ij}^{\omega} d_i^\dagger d_j + \text{h.c.} + U \sum_i n_i^d n_{i\#}^d; \quad (1)$$

where d_i^\dagger is the creation operator of $3d$ electron with spin \uparrow at site i , $n_i^d = d_i^\dagger d_i$, the summations $\langle ij \rangle$, $\langle\langle ij \rangle\rangle$, and $\langle\langle\langle ij \rangle\rangle\rangle$ run over first, second, and third nearest-neighbor pairs, respectively, and the rest of the notation is standard. The on-site Coulomb energy U corresponds to the charge transfer energy of cuprates.

The schematic process of the RIXS for Cu K-edge is shown in Fig. 1 (a). An absorption of an incident photon with energy $\hbar\omega$, momentum \mathbf{K} , and polarization ϵ brings about the dipole transition of an electron from

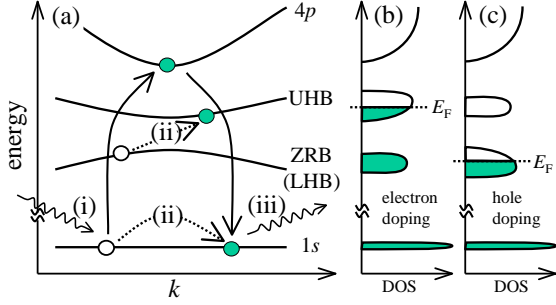


FIG. 1: Schematic picture of Cu K-edge RIXS process (a) and densities of states for electron- (b) and hole-doped (c) cases. The dipole transitions of an electron between 1s and 4p orbitals occur with (i) absorption and (iii) emission of a photon. The 3d electrons are excited (ii) in the intermediate state. The Fermi energies [denoted by dotted lines in (b) and (c)] are in UHB and ZRB (LHB) for electron- and hole-doped cases, respectively.

Cu 1s to 4p orbital [process (i)]. In the intermediate states, 3d electrons interact with a 1s-core hole and a photo-excited 4p electron via the Coulomb interactions so that the excitations in the 3d electron system are evolved [process (ii)]. The Fermi energies are located in the UHB and ZRB for electron- and hole-doped cases, respectively. As shown in (b) and (c) in Fig. 1, the excitations occur within the band as well as between the bands. The latter corresponds to the Mott gap excitation. The 4p electron in the intermediate state goes back to the 1s orbital again and a photon with energy ω_f , momentum \mathbf{K}_f , and polarization ϵ_f is emitted [process (iii)]. The differences of energies and momenta between incident and emitted photons are transferred to the 3d electron system.

In the intermediate states, there are a 1s-core hole and a 4p electron, with which 3d electrons interact. Since the 1s-core hole is localized in a small radius of the Cu 1s orbital, the attractive interaction between the 1s-core hole and 3d electrons is strong. The interaction is written as,

$$H_{1s-3d} = \sum_{i,j} U_c n_{i,j}^d n_{i,j}^s; \quad (2)$$

where $n_{i,j}^s$ is the number operator of 1s-core hole with spin \uparrow at site i , and U_c is taken to be positive. On the contrary, the Coulomb interactions related to the 4p electron are neglected since the 4p electron is delocalized [4]. Furthermore, we assume that the photo-excited 4p electron enters into the bottom of the 4p band with momentum \mathbf{k}_0 . Under these assumptions, the RIXS spectrum is expressed as,

$$I(\mathbf{K}; \omega) = \sum_{\mathbf{k}_0, \mathbf{k}_f} \sum_{\epsilon_f} \frac{1}{H(E_0 + \omega - \epsilon_f)} \langle \mathbf{j} | \mathbf{S}_{\mathbf{k}_0, \mathbf{k}_f}^y | \mathbf{i} \rangle \quad (3)$$

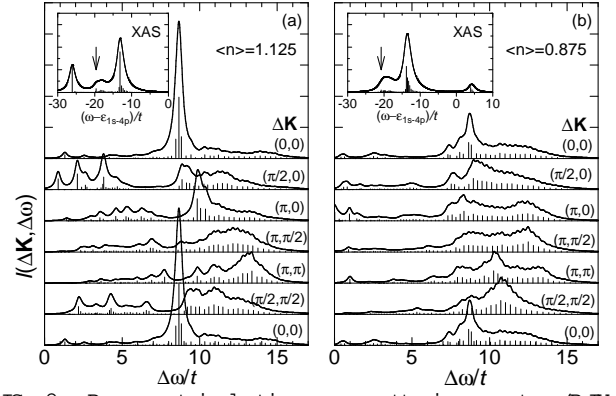


FIG. 2: Resonant inelastic x-ray scattering spectra (RIXS) for Cu K-edge of doped Hubbard model with long-range hoppings. (a) The electron doped case ($n_i = 1.125$). (b) The hole doped case ($n_i = 0.875$). The spectra of the elastic scattering process at $\mathbf{K} = (0,0)$ are not shown. The parameters are $U/t = 10$, $U_c/t = 15$, $t/t^0 = 1$, $t^0/t = 0.34$, and $t^0/t = 0.23$. The δ -functions (the vertical thin solid lines) are convoluted with Lorentzian broadening of $0.2t$. Insets are the Cu 1s absorption spectra with $\chi_{AS} = t/t^0 = 1.0$, and the incident photon energies ω_i 's for RIXS are set to the values denoted by the arrows.

where $H = H_{3d} + H_{1s-3d} + H_{1s;4p}$, $H_{1s;4p}$ being composed of the energy separation ϵ_{1s-4p} between the 1s level and the bottom of the 4p band, $\mathbf{K} = \mathbf{K}_i - \mathbf{K}_f$, $\epsilon = \epsilon_i - \epsilon_f$, $\mathbf{S}_{\mathbf{k}_0, \mathbf{k}_f}^y$ ($\mathbf{p}_{\mathbf{k}_0}^y$) is the creation operator of the 1s-core hole (4p electron) with momentum \mathbf{k} and spin \uparrow , $|\mathbf{j}\rangle$ is the ground state with energy E_0 , $|\mathbf{i}\rangle$ is the final state of the RIXS process with energy E , and δ is the inverse of the relaxation time in the intermediate state. The RIXS spectrum of Eq. (3) is calculated on a 4×4 -site cluster with periodic boundary conditions by using a modified version of the conjugate-gradient method together with the Lanczos technique.

The values of the parameters are as follows: $t^0/t = 0.34$, $t^0/t = 0.23$, $U/t = 10$, $U_c/t = 15$, and $t/t^0 = 1$ with $t = 0.35$ eV that are estimated from the analyses of ARPES data [12] and are the same as those used in Ref. [4].

Insets of Figs. 2 (a) and (b) are the Cu 1s x-ray absorption spectrum (XAS) for electron- and hole-doped cases, respectively. The spectrum is given by,

$$D(\omega) = \frac{1}{\pi} \text{Im} \langle \mathbf{j} | \mathbf{p}_{\mathbf{k}_0}^y \mathbf{S}_{\mathbf{k}_0, \mathbf{k}_f}^y | \mathbf{i} \rangle \frac{1}{H(E_0 + \omega - \epsilon_i)} \quad (4)$$

where H is the same as that in Eq. (3). In the inset of Fig. 2 (a), there appear three peaks, i.e., peaks at around $\epsilon_{1s-4p} = 26t$, $20t$, and $13t$. The peaks at around $20t$ and $13t$ are also seen in the undoped case [4]. The peak at around $20t$ corresponds to a final state where the core-hole is screened and thus the core-hole site is doubly occupied by 3d electrons ($U - 2U_c = 20t$). This final state promotes the excitations from LHB to UHB

in the RIXS. The peak at around $13t$ represents un-screened core-hole state and mainly contains the configuration that a core-hole is created at a singly occupied site ($U_c = 15t$). The peak at around $26t$, which appears upon electron-doping, corresponds to a final state where the core-hole is created at a doubly occupied site induced by doped electrons ($2U_c = 30t$). In the hole-doped case in Fig. 2 (b), a peak appears at around $4t$, in addition to the peaks at $20t$ and $13t$. The $4t$ peak mainly contains the configuration that the core-hole is created at an empty site induced by doped holes. Because we are interested in the excitations from LHB to UHB in the RIXS spectra, we set ω_i 's to the energy of the $20t$ peak as denoted by the arrows in the insets of Figs. 2 (a) and (b).

Figure 2 (a) shows the RIXS spectra in the electron-doped case ($n_i = 1.125$, where n_i is the electron concentration per site). The spectra below $8t$ are associated with the excitations within the UHB, and those above $8t$ are due to the excitations from LHB to UHB, i.e., Mott gap excitations. We note that, when the incident energy ω_i is set to $26t$ which is the lowest peak-energy in XAS, there is almost no Mott gap excitation and the RIXS spectra appear only in the lower energy region below $8t$ (not shown). This is because the excitation from a singly occupied state to a doubly occupied state is reduced in the intermediate state of the RIXS process. Therefore, by tuning ω_i to a peak energy of $U - 2U_c = 20t$, we can enhance strongly the RIXS spectra associated with the excitation from LHB to UHB ($\omega_i > 8t$). Since there is no such an enhancement effect of the Mott gap excitation in the optical conductivity [10, 11] as well as electron-energy loss spectroscopy, we can say that RIXS is the unique technique to investigate the Mott gap excitation even in doped materials. In the energy region above $8t$ in RIXS, the spectra strongly depend on momentum, showing a feature that the spectral weight shifts to higher energy region with increasing jK_j . The feature is similar to that of undoped case [4].

Figure 2 (b) shows the RIXS spectra in the hole-doped case ($n_i = 0.875$). The spectra above the energy $6t$ are due to the excitations from LHB to UHB. Compared with the electron-doped case, the spectra show broad features: For example, at $K = (\pi, \pi)$, the spectrum extends from $7t$ to $14t$, and the energy position of the maximum spectral weight ($10t$) is lower than that of electron-doped case ($13t$). The spectra at other K 's are also extended to wide energy region similar to that at (π, π) , and the energy positions of maximum spectral weights seem to be rather independent of momentum.

In order to compare the energy positions of the spectra, the momentum dependence of the center of gravity of the RIXS spectra associated with the excitation from LHB to UHB is plotted in Fig. 3. The spectral weight is adopted from the energy regions above $4t$, $8t$, and $6t$ for undoped ($n_i = 1$, denoted by circles in Fig. 3) [4], electron- (1.125, upward triangles), and hole-doped (0.875, down-

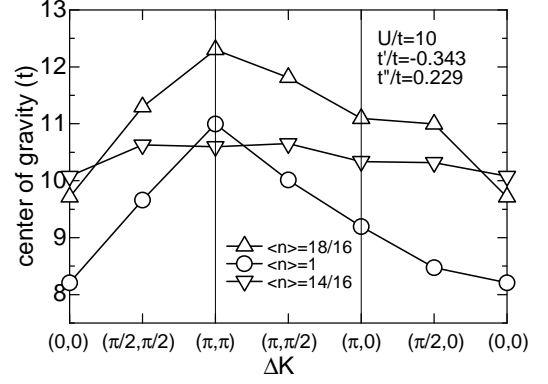


FIG. 3: Momentum dependence of the center of gravity of RIXS spectra associated with the excitation from LHB to UHB. The spectral weight is adopted in energy regions above $4t$, $8t$, and $6t$ for undoped ($n_i = 1$, denoted by circles), electron- (1.125, upward triangles), and hole-doped (0.875, downward triangles) cases, respectively.

ward triangles) cases, respectively. We find that the energy positions are shifted to the high energy side compared with that for the undoped case. This is because, upon hole- (electron-) doping, the Fermi energy shifts to LHB (UHB) and the energy difference between states of the occupied LHB and unoccupied UHB becomes large. In the undoped case of Fig. 3, the center of gravity shifts to higher energy with increasing jK_j . This momentum dependence remains by electron-doping, except along the $h1;0i$ direction where the energy difference between $(\pi/2, 0)$ and $(0, 0)$ is larger than that in undoped case. The origin of the similarity of the momentum dependence will be discussed below. Here let us discuss the physics behind the behavior of the $h1;0i$ direction. In undoped case, the RIXS spectra have a characteristic feature along the $h1;0i$ direction where the edge of the RIXS spectrum at $K = (\pi/2, 0)$ is rather lower in energy than that at $(0, 0)$ [4]: The edge of the RIXS at $K = (\pi/2, 0)$ comes from the excitation from the occupied $k = (\pi/2, 0)$ state to the unoccupied $k = (\pi, 0)$ one which is the lowest in energy in UHB [4]. This edge feature restrains the center of gravity at $(\pi/2, 0)$ from shifting to the higher energy in the undoped case. Since the $(\pi, 0)$ state of UHB is occupied by electrons upon electron-doping, the center of gravity at $K = (\pi/2, 0)$ in the RIXS shifts to the higher energy.

In contrast, the momentum dependence becomes weaker by hole-doping, as seen in Fig. 3. Let us make clear that the difference between electron- and hole-dopings comes from the lack of particle-hole symmetry in cuprates but not from the RIXS process itself in which the background configurations around the core-hole screened site are different between electron- and hole-dopings. In Fig. 4, plotted is the center of gravity of RIXS spectrum on the Hubbard model with the nearest neighbor hopping, which has the particle-hole symmetry. To obtain the RIXS spectra, the incident photon energies ω_i 's are set to be the energy at the peak of $U - 2U_c$ in XAS

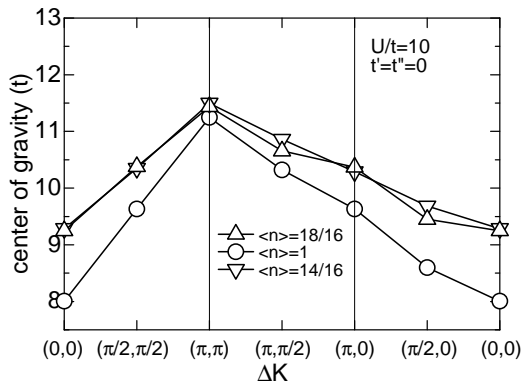


FIG. 4: The same as Fig. 3 but for $t^0 = t'' = 0$. The spectral weight is adopted in energy regions above $6t$, $7t$, and $7t$ for undoped, electron-, and hole-doped cases, respectively.

spectra for both electron- and hole-doped cases. We can obtain almost the same momentum dependence in both electron- and hole-dopings accompanied by the same energy shift from the undoped case, although the configurations in the intermediate states are different. Therefore, the excitation spectra from LHB to UHB have almost the same features between electron- and hole-doping when the model has the particle-hole symmetry.

One possible reason of the difference between electron- and hole-doping comes from the doping effect on the AF correlations. In the undoped case, it has been discussed that the AF correlation plays a crucial role in the RIXS excitation [4, 5]: The matrix elements of the excitation from the top of the LHB [$k = (\pi/2, \pi/2)$] to the bottom of the UHB [$k = (\pi, 0)$] are almost zero due to the coherence factor arising from the AF order. This fact affects strongly the momentum dependence of RIXS in the undoped case. Upon doping, the AF correlation changes. However, it strongly depends on carriers in the presence of the second and third nearest neighbor hoppings [13, 14, 15]: With the parameters used in Fig. 2, the short-range AF correlation is kept in electron-doped case, whereas the correlation is strongly suppressed in the hole-doped case. Thus, we can suppose that the RIXS spectra in electron-doped system is similar to the undoped case, while the spectra in hole-doped system

is different. In fact, as discussed above, in the case of electron-doping, the calculated RIXS spectra show the momentum dependence similar to that of the undoped case, but remarkably different in the case of hole-doping. Therefore, it is natural to consider that the Mottn gap excitation is significantly influenced by the magnitude of AF correlations even in doped systems.

Finally, we discuss the material dependence of RIXS. The parameters of the second and third nearest neighbor hoppings, t^0 and t'' , play a role in the material dependence of the electronic properties. The hopping parameters t^0 and t'' in LSCO are smaller than those in $\text{Bi}_2\text{Sr}_2\text{CaCu}_2\text{O}_8$ (BSCCO), $\text{Ca}_2\text{CuO}_2\text{Cl}_2$ (CCOC), and NCCO [16]. Therefore the features of the RIXS spectra on BSCCO, CCOC and NCCO are expected to follow Fig. 3 [17], while for doped LSCO, the feature may be rather similar to that in Fig. 4 [18].

In summary, we have demonstrated theoretically the difference of the Cu K-edge RIXS between hole- and electron-doped cuprates by using the numerically exact diagonalization technique on small clusters of the single-band Hubbard model with long-range hoppings. We have found that, upon electron-doping, the RIXS spectra along the $(\pi, 0)$ direction shift to the higher energy side than those in undoped case. In contrast to electron-doped case, the spectra for the excitations from the lower to upper Hubbard bands show the broad feature and less momentum dependence in the hole-doped case. The difference in the spectra between hole- and electron-doped systems may be due to the different behavior of short-range AF spin correlation in the doped systems. The RIXS experiments in a variety of doped cuprates are desired [17, 18].

The authors would like to thank M. Z. Hasan, J. P. Hill, and Y. J. Kim for informing their experimental data prior to publication and for valuable discussions. The numerical calculations in Fig. 2 are assisted by H. Kondo. This work was supported by Priority-A Grants from the Ministry of Education, Science, Culture and Sport of Japan and CREST. Computations were carried out in ISSP, University of Tokyo; IMR, Tohoku University; and Tohoku University.

-
- [1] M. Z. Hasan et al., *Science* **288**, 1811 (2000).
 - [2] Y. J. Kim et al., *Phys. Rev. Lett.* **89**, 177003 (2002).
 - [3] F. C. Zhang and T. M. Rice, *Phys. Rev. B* **37**, 3759 (1988).
 - [4] K. Tsuchi et al., *Phys. Rev. Lett.* **83**, 3705 (1999).
 - [5] K. Tsuchi et al., *Advances in Superconductivity X II*, Springer-Verlag, Tokyo, 197 (2000).
 - [6] M. Z. Hasan et al., *Phys. Rev. Lett.* **88**, 177403 (2002).
 - [7] K. Tsuchi et al., *Phys. Rev. B* **61**, 7180 (2000).
 - [8] H. Takagi et al., *Physica C* **162-164**, 1001 (1989).
 - [9] A. Damascelli et al., *Rev. Mod. Phys.* in press.
 - [10] S. Uchida et al., *Phys. Rev. B* **43**, 7942 (1991).
 - [11] T. Arita et al., *Phys. Rev. B* **48**, 6597 (1993).
 - [12] C. Kim et al., *Phys. Rev. Lett.* **80**, 4245 (1998).
 - [13] T. Tohyama and S. Maekawa, *Phys. Rev. B* **49**, 3596 (1994).
 - [14] R. J. Gooding, K. J. E. Vos, and P. W. Leung, *Phys. Rev. B* **50**, 12 866 (1994).
 - [15] T. Tohyama and S. Maekawa, *Phys. Rev. B* **64**, 212505 (2001).
 - [16] T. Tohyama and S. Maekawa, *Phys. Rev. B*, in press (2003).
 - [17] M. Z. Hasan, private communications.
 - [18] Y. J. Kim and J. P. Hill, private communications.